

Phase transitions in the one-dimensional ionic Hubbard model

Myung-Hoon Chung*

College of Science and Technology, Hongik University, Sejong 339-701, Korea

(Dated: February 19, 2022)

We study quantum phase transitions by measuring the bond energy, the number density, and the half-chain entanglement entropy in the one-dimensional ionic Hubbard model. By performing the infinite density matrix renormalization group with matrix product operator, we obtain ground states as the canonical form of matrix product states. Depending on the chemical potential and the staggered potential, the number density and the half-chain entanglement entropy shows clear signatures of the Mott transition. Our results confirm the success of the matrix product operator method for investigation of itinerant fermion systems.

I. INTRODUCTION

Intrinsic characteristics of quantum entanglements [1, 2] are essential elements in the study of quantum phase transitions [3]. In recent years, there has been a great deal of interest in entanglement entropy [4], which is a quantum phase transition marker [5] in the interacting spin [6–8], boson [9], and fermion [10–13] systems.

Some cold atoms can obey the same statistical rules as electrons if atoms with an odd number of neutrons are fermions [14]. Thus, some cold atoms [15] in an optical lattice can mimic the behavior of electrons in a real solid material. Since cold fermion systems are invented in quasi one-dimensional optical lattices [16], the one-dimensional fermion Hubbard model can be realized physically. The one-dimensional fermion Hubbard model [17] was analytically solved and became a prototype of a playground, where theoretical results could be compared to physical reality.

In this paper, motivated by cold atoms, we study the one-dimensional Hubbard model with an energy offset between even and odd lattice sites. The main process in this study aims to see the role of different potential energies, which is made by the second laser disturbance in the one-dimensional cold atom systems. In fact, we impose the potential energy as

$$V(x) = V_\lambda \sin(kx) + V_{2\lambda} \sin\left(\frac{k}{2}x\right), \quad (1)$$

using the second laser of the doubly long wavelength. For example, we present the staggered potential with typical values as shown in Fig. 1.

The ionic Hubbard model [18] stemmed from this staggered potential. There have been many investigations into the ionic Hubbard model at half filling, by using dynamical mean field theory [19, 20], determinant quantum Monte Carlo [21], exact diagonalization and finite density matrix renormalization group [22].

The purpose of this paper is to find a quantum phase diagram in the one-dimensional ionic Hubbard model

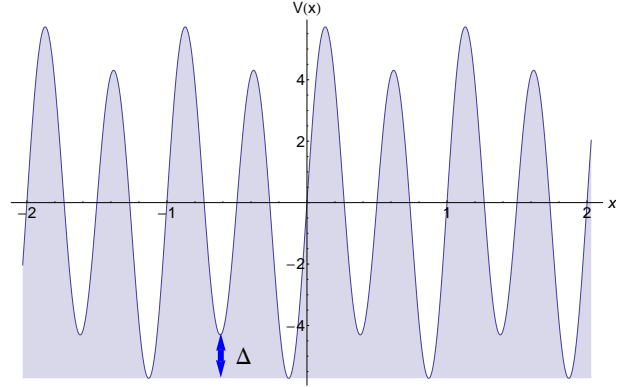


FIG. 1: The shape of the potential energy made by two wavelength lasers λ and 2λ . Explicitly, we plot $V(x) = 5 \sin(4\pi x) + \sin(2\pi x)$. We notice the staggered potential Δ .

away from half filling. To do this, we propose the ansatz of matrix product state (MPS) for the ground state, and perform the infinite density matrix renormalization group (iDMRG) [23] method with matrix product operator (MPO). By changing the chemical potential and the staggered potential, we calculate the entanglement entropy, which shows quantum phase transition. The occupation number density also indicates the transition consistently. We determine the phase diagram in the parameter space.

II. MODEL AND METHOD

Introducing the staggered one-particle potential Δ into the Hubbard model, we consider a simple quantum system of interacting fermions on a one-dimensional lattice. The Hamiltonian for this model is written as

$$\begin{aligned} H = & -t \sum_{\langle ij \rangle} (c_{i\uparrow}^\dagger c_{j\uparrow} + c_{j\uparrow}^\dagger c_{i\uparrow} + c_{i\downarrow}^\dagger c_{j\downarrow} + c_{j\downarrow}^\dagger c_{i\downarrow}) \\ & + U \sum_i (n_{i\uparrow} - \frac{1}{2})(n_{i\downarrow} - \frac{1}{2}) - \mu \sum_i (n_{i\uparrow} + n_{i\downarrow}) \\ & + \frac{\Delta}{2} \sum_{i \in \text{Even}} (n_{i\uparrow} + n_{i\downarrow}) - \frac{\Delta}{2} \sum_{i \in \text{Odd}} (n_{i\uparrow} + n_{i\downarrow}), \quad (2) \end{aligned}$$

*mhchung@hongik.ac.kr

where $\langle ij \rangle$ represents the nearest-neighbor hopping in a one-dimensional lattice, and $n_{i\uparrow}$ and $n_{i\downarrow}$ are the spin-up and the spin-down number operator, respectively. We let the hopping strength t be 1 and vary the strengths of the parameters: the on-site Coulomb repulsion U , the chemical potential μ , and the staggered potential Δ . The role of the chemical potential is to control the number of fermions in the system. For the case of $\Delta = 0$, the exact solution of the original Hubbard model is known [24].

In order to handle μ and Δ , we introduce two linear combinations μ_e and μ_o for even and odd sites, denoting

$$\mu_e \equiv \mu - \frac{\Delta}{2}, \quad \mu_o \equiv \mu + \frac{\Delta}{2}. \quad (3)$$

Because the Hamiltonian has the two-site translational symmetry as shown in Fig. 1, we apply iDMRG with unit cell of two sites to determine the ground state. Our strategy is to use MPO acting on MPS.

In relation to the basis, we set the physical index σ_i in the MPS. The state on the i -th site is represented by $\sigma_i = (\alpha_i, \beta_i)$, such as $0 = (0, 0)$ for the empty, $1 = (0, 1)$ for the spin-down, $2 = (1, 0)$ for the spin-up, and $3 = (1, 1)$ for both of the spin-up and the spin-down. Thus, the physical index runs from 0 to 3. The basis of the Fock space is written in terms of creation operators $c_{i\uparrow}^\dagger$ and $c_{i\downarrow}^\dagger$ as follows:

$$|\sigma_0 \cdots \sigma_{L-1}\rangle = (c_{0\uparrow}^\dagger)^{\alpha_0} (c_{0\downarrow}^\dagger)^{\beta_0} (c_{1\uparrow}^\dagger)^{\alpha_1} (c_{1\downarrow}^\dagger)^{\beta_1} \cdots (c_{L-1\uparrow}^\dagger)^{\alpha_{L-1}} (c_{L-1\downarrow}^\dagger)^{\beta_{L-1}} |0\rangle, \quad (4)$$

where $\alpha_i(\beta_i) = 0$ or 1 means that there is a spin-up (down) fermion vacancy or occupancy at the i -th site, respectively. It is important to maintain the order of fermions in the state of the Fock space to deal with the negative sign caused by fermion exchange. We adopt the order of spin-up first and then spin-down as described above.

In the process of iDMRG, we have to find the MPO for the Hamiltonian of Eq. (2). We convince that the MPO of the i -th site is indeed given by the following form:

$$M_i = \begin{pmatrix} 1 & c_{i\uparrow}^\dagger & c_{i\downarrow}^\dagger & c_{i\uparrow} & c_{i\downarrow} & b_i \\ 0 & 0 & 0 & 0 & 0 & -tc_{i\uparrow} \\ 0 & 0 & 0 & 0 & 0 & -tc_{i\downarrow} \\ 0 & 0 & 0 & 0 & 0 & tc_{i\uparrow}^\dagger \\ 0 & 0 & 0 & 0 & 0 & tc_{i\downarrow}^\dagger \\ 0 & 0 & 0 & 0 & 0 & 1 \end{pmatrix} \quad (5)$$

where

$$b_i = U(n_{i\uparrow} - \frac{1}{2})(n_{i\downarrow} - \frac{1}{2}) - \bar{\mu}(n_{i\uparrow} + n_{i\downarrow}), \quad (6)$$

$$\bar{\mu} = \begin{cases} \mu_e & \text{for } i = \text{even}, \\ \mu_o & \text{for } i = \text{odd}. \end{cases} \quad (7)$$

Here, we omit to present the boundary operators. We note that the MPO for even sites is slightly different from

the MPO for odd sites, where μ_e must be replaced with μ_o . Because c and c^\dagger are fermion operators, the commutation relations between M_i and $c_{j\sigma}^\dagger$ ($i \neq j$, $\sigma = \uparrow, \downarrow$) are given by $M_i c_{j\sigma}^\dagger = c_{j\sigma}^\dagger M_i^*$, where

$$M_i^* = \begin{pmatrix} 1 & -c_{i\uparrow}^\dagger & -c_{i\downarrow}^\dagger & -c_{i\uparrow} & -c_{i\downarrow} & b_i \\ 0 & 0 & 0 & 0 & 0 & tc_{i\uparrow} \\ 0 & 0 & 0 & 0 & 0 & tc_{i\downarrow} \\ 0 & 0 & 0 & 0 & 0 & -tc_{i\uparrow}^\dagger \\ 0 & 0 & 0 & 0 & 0 & -tc_{i\downarrow}^\dagger \\ 0 & 0 & 0 & 0 & 0 & 1 \end{pmatrix} \quad (8)$$

When the Hamiltonian acts on the basis, the sign caused by fermion exchange must be taken care of such as

$$\begin{aligned} & M_0 \cdots M_{L-1} (c_{0\uparrow}^\dagger)^{\alpha_0} (c_{0\downarrow}^\dagger)^{\beta_0} (c_{1\uparrow}^\dagger)^{\alpha_1} (c_{1\downarrow}^\dagger)^{\beta_1} \\ & \cdots (c_{L-1\uparrow}^\dagger)^{\alpha_{L-1}} (c_{L-1\downarrow}^\dagger)^{\beta_{L-1}} |0\rangle \\ & = M_0 (c_{0\uparrow}^\dagger)^{\alpha_0} (c_{0\downarrow}^\dagger)^{\beta_0} \bar{M}_1 (c_{1\uparrow}^\dagger)^{\alpha_1} (c_{1\downarrow}^\dagger)^{\beta_1} \cdots \\ & \bar{M}_{L-1} (c_{L-1\uparrow}^\dagger)^{\alpha_{L-1}} (c_{L-1\downarrow}^\dagger)^{\beta_{L-1}} |0\rangle, \end{aligned} \quad (9)$$

where the total number of fermions in the left side of the i -th site, $N_i \equiv \sum_{k=0}^{i-1} (\alpha_k + \beta_k)$, determines the 6×6 matrix:

$$\bar{M}_i = \begin{cases} M_i & \text{for } N_i = \text{even}, \\ M_i^* & \text{for } N_i = \text{odd}. \end{cases} \quad (10)$$

In order to manage the sequence of Eq. (9), we note that the even and odd structure of the fermion numbers (E O) is kept recursively by $e \equiv \{|0\rangle, c_{\uparrow}^\dagger c_{\downarrow}^\dagger |0\rangle\}$ and $o \equiv \{c_{\uparrow}^\dagger |0\rangle, c_{\downarrow}^\dagger |0\rangle\}$ such as

$$\begin{aligned} (E \ O) & \begin{pmatrix} e & o \\ o & e \end{pmatrix} \begin{pmatrix} e & o \\ o & e \end{pmatrix} \cdots \begin{pmatrix} e & o \\ o & e \end{pmatrix} \\ & = (E \ O) \begin{pmatrix} e & o \\ o & e \end{pmatrix} \cdots \begin{pmatrix} e & o \\ o & e \end{pmatrix}. \end{aligned} \quad (11)$$

Using the relation of Eq. (11), we double the MPO for the i -th site, \bar{M}_i , which is modified into 12×12 matrix, D_i , such as

$$D_i e = \begin{pmatrix} M_i e & 0 \\ 0 & M_i^* e \end{pmatrix}, \quad D_i o = \begin{pmatrix} 0 & M_i o \\ M_i^* o & 0 \end{pmatrix}, \quad (12)$$

where M_i^* is used in the second row because there are odd number of fermions in the left side of the i -th site. By including the 4-dimensional physical index, we present the effective MPO as the graphical diagram with the four-leg tensor D having $4 \times 12 \times 12 \times 4$ elements, of which the number of non-zero elements is small:

$$\cdots - \begin{array}{c} | \\ D \\ | \end{array} - \begin{array}{c} | \\ D \\ | \end{array} - \begin{array}{c} | \\ D \\ | \end{array} - \cdots \quad (13)$$

It is remarkable that the so-called fermionic matrix product states [25] are introduced in a similar fashion of doubling the MPO. We have already tested this MPO approach [26], and the numerical results by doubling the

MPO were compared with those obtained by the Jordan-Wigner transformation in good agreement.

By adopting the two-site iDMRG algorithm, we optimize two tensors in our MPS, A_{ab}^σ and B_{ab}^σ . The physical index σ takes a value of 0 to 3, and the indices a (left) and b (right) run from 0 to $\chi - 1$, where χ is the internal bond dimension. The Schmidt coefficients are denoted by λ_b^{AB} between A_{ab}^σ and B_{bc}^ρ , and by λ_b^{BA} between B_{ab}^σ and A_{bc}^ρ . A state in the MPS space is represented by graphic notation such as

$$\dots - \overset{|}{A} - \lambda^{AB} - \overset{|}{B} - \lambda^{BA} - \overset{|}{A} - \dots \quad (14)$$

By evaluating $4 \times 12 \times 12 \times 4$ elements of D , we perform iDMRG by acting the MPO of Eq. (13) on the MPS of Eq. (14). Regardless of the values of t , U , μ_e , and μ_o used in our calculations, we have observed a smooth convergence. Our numerical iDMRG results show that the ground-state solutions are divided into two classes: the MPS are either of the form $\dots ABABAB \dots$, which we will identify as a Mott phase with unit cell of two sites, near half filling, or uniform $\dots AAAAAA \dots$, which we will identify as metallic, further away from half filling.

III. NUMERICAL RESULTS

By setting $t = 1$ and $U = 4$, for a given μ_e and μ_o , we calculate the ground state by the two-site iDMRG. With the ground state, we extract three physical quantities corresponding to even and odd sites: the bond energy $\langle h_e \rangle$ and $\langle h_o \rangle$, the number density $\langle n_e \rangle$ and $\langle n_o \rangle$, and the half-chain entanglement entropy S_e and S_o . Here, the bond Hamiltonian h_e ($i = \text{even}$) is written as

$$\begin{aligned} h_e = & -t(c_{i\uparrow}^\dagger c_{j\uparrow} + c_{j\uparrow}^\dagger c_{i\uparrow} + c_{i\downarrow}^\dagger c_{j\downarrow} + c_{j\downarrow}^\dagger c_{i\downarrow}) \\ & + \frac{U}{2}(n_{i\uparrow} - \frac{1}{2})(n_{i\downarrow} - \frac{1}{2}) - \frac{\mu_e}{2}(n_{i\uparrow} + n_{i\downarrow}) \\ & + \frac{U}{2}(n_{j\uparrow} - \frac{1}{2})(n_{j\downarrow} - \frac{1}{2}) - \frac{\mu_o}{2}(n_{j\uparrow} + n_{j\downarrow}). \end{aligned} \quad (15)$$

Also, the occupation number density operator n_e ($i = \text{even}$) is written as

$$n_e = n_{i\uparrow} + n_{i\downarrow} = c_{i\uparrow}^\dagger c_{i\uparrow} + c_{i\downarrow}^\dagger c_{i\downarrow}. \quad (16)$$

Using the Schmidt coefficients λ_a between A and B in the MPS, we determine S_e . Keeping the normalization with $\sum_{a=0}^{\chi-1} \lambda_a^2 = 1$, we calculate the half-chain entanglement entropy S_e , which is given by

$$S_e = - \sum_{a=0}^{\chi-1} \lambda_a^2 \log_2 \lambda_a^2. \quad (17)$$

Obviously, we choose $i = \text{odd}$ for h_o and n_o . We use the Schmidt coefficients λ^{BA} between B and A in the MPS for S_o .

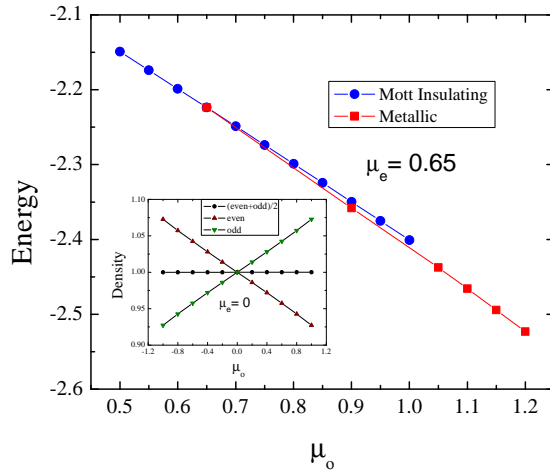


FIG. 2: Ground-state bond energy $(\langle h_e \rangle + \langle h_o \rangle)/2$ versus μ_o showing a level-crossing between Mott-insulating and metallic solutions, at $\mu_e = 0.65$ and $\chi = 100$. We set $t = 1$ and $U = 4$. Inset: the number density of $\langle n_e \rangle$, $\langle n_o \rangle$ and $(\langle n_e \rangle + \langle n_o \rangle)/2$ versus μ_o showing the Mott-insulating states, at $\mu_e = 0$ and $\chi = 100$. Although the difference of $(\langle n_e \rangle - \langle n_o \rangle)$ increases as the staggered potential $\Delta = (\mu_o - \mu_e)$ becomes bigger, the average number density $(\langle n_e \rangle + \langle n_o \rangle)/2$ remains fixed as 1 in the Mott-insulating states.

In order to verify the correctness of the calculation, we use an important analytic result [17] from the critical point of μ_+ at which the Mott insulator - metallic phase transition takes place in the restricted parameter space of $\mu_e = \mu_o$ or $\Delta = 0$. In fact, the transition point μ_+ is given by

$$\mu_+ = -2 + \frac{U}{2} + 2 \int_0^\infty \frac{d\omega}{\omega} \frac{J_1(\omega) \exp(-\omega U/4)}{\cosh(\omega U/4)}. \quad (18)$$

For $U = 4$, we obtain the exact critical point, $\mu_+ = \mu_e = \mu_o = 0.643364$. We present the average bond energy $(\langle h_e \rangle + \langle h_o \rangle)/2$ as shown in Fig. 2, where the level-crossing takes place at $\mu_e = \mu_o \sim 0.65$.

In Fig. 2, to determine the level-crossing of the average bond energy, we compute the ground state starting from $\mu_o = 0$. On the other hand, we can also calculate the ground state of the uniform solution by decreasing μ_o from large values. In each iDMRG calculation, the tensors of the initial environment are given by the previous solution of the different μ_o .

In order to determine the Mott transition in the parameter space of μ_e and μ_o , we compute the average number density $(\langle n_e \rangle + \langle n_o \rangle)/2$ and the average entanglement entropy $(S_e + S_o)/2$. Fixing μ_o , we present $(\langle n_e \rangle + \langle n_o \rangle)/2$ and $(S_e + S_o)/2$ by varying μ_e , as shown in Fig. 3 and 4. We note that the abrupt behaviour corresponds to the Mott transition.

As the main numerical result, we present the phase diagram in Fig. 5. One notices the robustness of the Mott state. In fact, we find that a small difference of

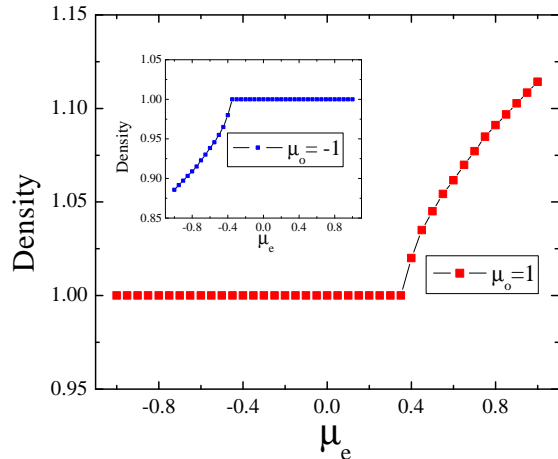


FIG. 3: The number density $(\langle n_e \rangle + \langle n_o \rangle)/2$ versus μ_e showing the abrupt change near $\mu_e = 0.35$, at $\mu_o = 1$, by setting $t = 1$, $U = 4$ and $\chi = 100$. We note that the phase transition takes place near $\mu_e = 0.35$. Inset: By setting $\mu_o = -1$, the number density versus μ_e showing the phase transition near $\mu_e = -0.35$.

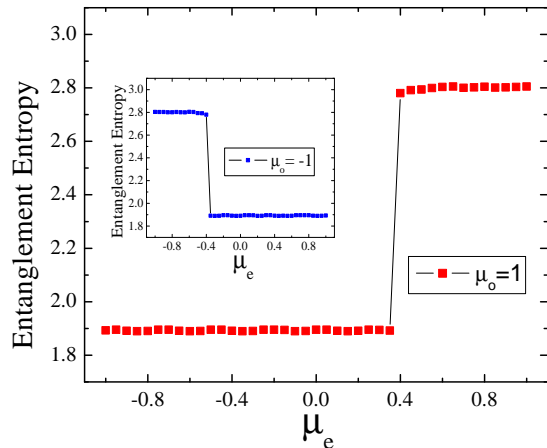


FIG. 4: The half-chain entanglement entropy $(S_e + S_o)/2$ versus μ_e showing the jump near $\mu_e = 0.35$, at $\mu_o = 1$, by setting $t = 1$, $U = 4$ and $\chi = 100$. We note that the phase transition takes place near $\mu_e = 0.35$. Inset: By setting $\mu_o = -1$, the half-chain entanglement entropy versus μ_e showing the phase transition near $\mu_e = -0.35$.

energy offsets, which is the staggered potential $\Delta = \mu_o - \mu_e$, can not destroy the Mott phase.

IV. CONCLUSION

In summary, we have used iDMRG with MPO to obtain the ground state in the one-dimensional ionic Hub-

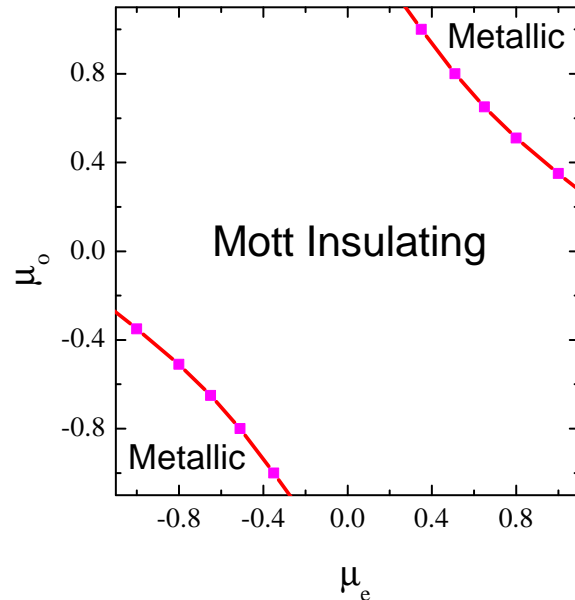


FIG. 5: Numerical phase diagram of the one-dimensional ionic Hubbard model. We have set $t = 1$ and $U = 4$. In the region of the Mott-insulating phase, the number density is given by 1, and the entanglement entropy is almost a constant. The red line is a guide to the eyes. The region of the Mott-insulating phase shrinks for smaller U .

bard model. We calculate the occupation number density and the half-chain entanglement entropy to determine the Mott transition. We draw the phase diagram in the two-dimensional parameter space of the chemical potential and the staggered potential.

It is of interest to extend our method to manage the number of fermions in two-dimensional systems. A typical topic of interest may be the two-dimensional fermion Hubbard model, for which our first task is to build a local tensor product operator like MPO. Although we do not encounter the notorious sign problem here, we should overcome the sign problem in the two-dimensional Hubbard model with the tensor product operator. As we double MPO as explained above, we can double the tensor product operator in order to support the number of fermions. We anticipate progress in the two-dimensional case.

Acknowledgments

This work was partially supported by the Basic Science Research Program through the National Research Foundation of Korea (NRF) funded by the Ministry of Education, Science and Technology (Grant No. NRF-2017R1D1A1A0201845). The author would like to thank M. C. Cha for helpful discussions.

-
- [1] A. Osterloh, L. Amico, G. Falci, and R. Fazio, *Nature* **416**, 608 (2002).
- [2] T. J. Osborne and M. A. Nielsen, *Phys. Rev. A* **66**, 032110 (2002).
- [3] S. Sachdev, *Quantum Phase Transitions* (Cambridge University Press, 2011).
- [4] J. Eisert, M. Cramer, and M. B. Plenio, *Rev. Mod. Phys.* **82**, 277 (2010).
- [5] M. C. Cha and M. H. Chung, *Physica B* **536**, 701 (2018).
- [6] L. Tagliacozzo, T. R. de Oliveira, S. Iblisdir, and J. I. Latorre, *Phys. Rev. B* **78**, 024410 (2008).
- [7] F. Pollmann, A. M. Turner, E. Berg, and M. Oshikawa, *Phys. Rev. B* **81**, 064439 (2010).
- [8] B. Pirvu, G. Vidal, F. Verstraete, and L. Tagliacozzo, *Phys. Rev. B* **86**, 075117 (2012).
- [9] M. Pino, J. Prior, A. M. Somoza, D. Jaksch, and S. R. Clark, *Phys. Rev. A* **86**, 023631 (2012).
- [10] S.-J. Gu, S.-S. Deng, Y.-Q. Li, and H.-Q. Lin, *Phys. Rev. Lett.* **93**, 086402 (2004).
- [11] D. Larsson and H. Johannesson, *Phys. Rev. Lett.* **95**, 196406 (2005).
- [12] F. Iemini, T. O. Maciel, and R. O. Vianna, *Phys. Rev. B* **92**, 075423 (2015).
- [13] M. C. Cha, *Phys. Rev. B* **98**, 235161 (2018).
- [14] M. F. Parsons, F. Huber, A. Mazurenko, C. S. Chiu, W. Setiawan, K. Wooley-Brown, and M. G. S. Blatt, *Phys. Rev. Lett.* **114**, 213002 (2015).
- [15] L. W. Cheuk, M. A. Nichols, M. Okan, T. Gersdorf, V. V. Ramasesh, W. S. Bakr, T. Lompe, and M. W. Zwierlein, *Phys. Rev. Lett.* **114**, 193001 (2015).
- [16] M. Schreiber, S. S. Hodgman, P. Bordia, H. P. Lüschen, M. H. Fischer, R. Vosk, E. Altman, U. Schneider, and I. Bloch, *Science* **21**, 842 (2015).
- [17] F. H. L. Essler, H. Frahm, F. Göhmann, A. Klümper, and V. E. Korepin, *The one-dimensional Hubbard model* (Cambridge University Press, 2005).
- [18] M. H. Torbati, N. A. Drescher, and G. S. Uhrig, *Phys. Rev. B* **89**, 245126 (2014).
- [19] S. Bag, A. Garg, and H. R. Krishnamurthy, *Phys. Rev. B* **91**, 235108 (2015).
- [20] H. F. Lin, H. D. Liu, H. S. Tao, and W. M. Liu, *Scientific Reports* **5**, 9810 (2015).
- [21] K. Bouadim, N. Paris, F. Hebert, G. G. Batrouni, and R. T. Scalettar, *Phys. Rev. B* **76**, 085112 (2007).
- [22] A. P. Kampf, M. Sekania, G. I. Japaridze, and P. Brune, *J of Phys.: Condensed Matter* **15**, 5895 (2003).
- [23] I. P. McCulloch, e-print arXiv:0804.2509 (2008).
- [24] C. Yang, A. N. Kocharian, and Y. L. Chiang, *J. Phys.: Condens. Matter* **12**, 7433 (2000).
- [25] N. Bultinck, D. J. Williamson, J. Haegeman, and F. Verstraete, *Phys. Rev. B* **95**, 075108 (2017).
- [26] M. H. Chung, E. Orignac, D. Poilblanc, and S. Capponi, e-print arXiv:1912.10203 (2019).